(pH 7.4) or 10 mM sodium acetate (pH 5.0) buffer. The sample solutions were incubated at ambient temperature overnight. The fluorescence intensity of the samples at $\lambda = 590$ nm (excitation at $\lambda = 510$ nm) was measured at 25 °C with a spectrofluorometer (FP-6500, Jasco, Tokyo, Japan). The relative fluorescence intensity was calculated as: $F_r = (F_{sample} - F_0)/(F_{100} - F_0)$, for which F_{sample}, F_{100}, and F_0 represent the fluorescence intensity of the samples, free pDNA, and background, respectively.

Dynamic light scattering (DLS) and ζ potential measurements: In the DLS measurements, polyplex solutions with various *N/P* ratios in 10 mM Tris–HCl buffer (pH 7.4) were adjusted to have pDNA concentrations of 33.3 $\mu g\,mL^{-1}$. DLS measurements were then performed at 25 ± 0.2 °C with a DLS-7000 instrument (Otsuka Electronics, Osaka, Japan) with a vertically polarized incident beam of $\lambda = 488$ nm from an Ar ion laser. The ζ potential of the polyplex micelles was measured at 25 ± 0.2 °C with an ELS-6000 instrument (Otsuka Electronics, Osaka, Japan) equipped with a He–Ne ion laser ($\lambda = 633$ nm). The scattering angle was fixed at 20°. From the obtained electrophoretic mobility, the ζ potential was calculated by using the Smoluchowski equation: $\zeta = 4\pi\eta\upsilon/\varepsilon$ in which η is the electrophoretic mobility, υ is the viscosity of the solvent, and ε is the dielectric constant of the solvent. The results are expressed as the average of five experiments.

In vitro transfection of HuH-7 cells: Human hepatoma HuH-7 cells were seeded on 6-well culture plates and incubated overnight in 1.5 mL Dulbecco's modified Eagle medium (DMEM) containing 10% fetal bovine serum (FBS) before transfection. The cells were then incubated with the polyplex micelles from PEG-*b*-P[Asp(EDA)], PEG-*b*-P[Asp(DET)], PEG-*b*-P[Asp(MDET)], and PEG-*b*-P[Asp(DEDET)] (3 μg pDNA/well) with various *N/P* ratios in DMEM containing 10% FBS for 24 h, followed by an additional incubation for 24 h in the absence of polyplexes. Luciferase gene expression was evaluated using the Luciferase Assay System (Promega, Madison, USA) and a Lumat LB9507 luminometer (Berthold Technologies, Bad Wildbad, Germany). The results were expressed as light units per milligram of cell protein determined by a BCA assay kit (Pierce, Rockford, USA).

Mouse primary osteoblast culture and transfection. Osteoblasts were isolated from calvariae of neonatal littermates. The experimental procedures were handled in accordance with the guidelines of the Animal Committee of the University of Tokyo. Calvariae were digested for 10 min at 37 °C in an enzyme solution containing 0.1% collagenase and 0.2% dispase for five cycles. Cells isolated by the final four digestions were combined as an osteoblast population and cultured in DMEM containing 10% FBS. For luciferase transfection assays, primary osteoblasts were inoculated at a density of 2×10^4 cells/well in a 24-multiwell plate, cultured for 24 h, and, after changing to fresh culture medium containing 10% FBS, pDNA polyplex solution (33.3 $\mu g\,mL^{-1}$, 22.5 μL) was applied to each well. Luciferase gene expression was measured 48 h later by using the Luciferase Assay System (Promega) and a Lumat LB9507 luminometer (Berthold). For the cytotoxicity assay, primary osteoblasts were plated into a 96-multiwell plate (6×10^3 cells/well). After 24 h incubation, 6 μL of each pDNA polyplex solution was added, followed by further incubation for 24 h. The viability of the cells was evaluated by an MTT assay (Cell Counting Kit-8, Dojindo, MTT = 3-[4,5-dimethylthiazol-2-yl]-2,5-diphenyltetrazolium bromide). Each well was measured by reading the absorbance at $\lambda = 450$ nm according to the protocol provided by the manufacturer.

Acknowledgements

The authors are grateful to the Health and Labor Sciences Research Grants in Research on Advanced Medical Technology in Nanomedicine Area from the Ministry of Health, Labor and Welfare (MHLW), Japan. They also express their thanks for the Grant-in-Aid for Scientific Research, the Special Coordination Funds for Promoting Science and Technology, and the Project on the Materials Development for Innovative Nano-Drug Delivery Systems from the Ministry of Education, Culture, Sports, Science and Technology (MEXT), Japan. The authors thank Professor Yukio Nagasaki and Dr. Motoi Oishi (University of Tsukuba) for use of the SEC instruments and their helpful suggestions, and Mr. Masataka Nakanishi for valuable discussions.

Keywords: aminolysis · block copolymers · gene delivery · polycations · polymeric micelles

[1] I. M. Verma, N. Somia, *Nature* **1997**, *389*, 239.
[2] M. Ogris, E. Wagner, *Drug Discovery Today* **2002**, *7*, 479.
[3] A. K. Salem, P. C. Searson, K. W. Leong, *Nat. Mater.* **2003**, *2*, 668.
[4] N. Nishiyama, A. Iriyama, W.-D. Jang, K. Miyata, K. Itaka, Y. Inoue, H. Takahashi, Y. Yanagi, Y. Tamaki, H. Koyama, K. Kataoka, *Nat. Mater.* **2005**, *4*, 934.
[5] S. O. Han, R. I. Mahato, S. W. Kim, *Bioconjugate Chem.* **2001**, *12*, 337.
[6] Y. Liu, L. Wenning, M. Lynch, T. M. Reineke, *J. Am. Chem. Soc.* **2004**, *126*, 7422.
[7] K. Itaka, K. Yamauchi, A. Harada, K. Nakamura, H. Kawaguchi, K. Kataoka, *Biomaterials* **2003**, *24*, 4495.
[8] K. Miyata, Y. Kakizawa, N. Nishiyama, A. Harada, Y. Yamasaki, H. Koyama, K. Kataoka, *J. Am. Chem. Soc.* **2004**, *126*, 2355.
[9] D. Wakebayashi, N. Nishiyama, Y. Yamasaki, K. Itaka, N. Kanayama, A. Harada, Y. Nagasaki, K. Kataoka, *J. Controlled Release* **2004**, *95*, 653.
[10] S. Fukushima, K. Miyata, N. Nishiyama, N. Kanayama, Y. Yamasaki, K. Kataoka, *J. Am. Chem. Soc.* **2005**, *127*, 2810.
[11] M. Harada-Shiba, K. Yamauchi, A. Harada, I. Takamisawa, K. Shimokado, K. Kataoka, *Gene Ther.* **2002**, *9*, 407.
[12] Y.-Y. Kim, H.-C. Chang, Y. T. Lee, U.-I. Cho, D. W. Boo, *J. Phys. Chem. A* **2003**, *107*, 5007.
[13] J.-P. Behr, *Chemia* **1997**, *51*, 34.
[14] V. Saudek, H. Pivcova, J. Drobnik, *Biopolymers* **1981**, *20*, 1615.
[15] A. V. Kabanov, T. K. Bronich, V. A. Kabanov, K. Yu, A. Eisenberg, *Macromolecules* **1996**, *29*, 6797.
[16] R. T. Franceschi, S. Yang, R. B. Rutherford, P. H. Krebsbach, M. Zhao, D. Wang, *Cells Tissues Organs* **2004**, *176*, 95–108.
[17] C. L. Gebhart, A. V. Kabanov, *J. Controlled Release* **2001**, *73*, 401.
[18] K. Itaka, N. Kanayama, N. Nishiyama, S. Fukushima, Y. Yamasaki, S. Oba, U.-I. Chung, H. Kawaguchi, K. Nakamura, K. Kataoka, *Proceedings of the 12th International Symposium on Recent Advances in Drug-Delivery Systems and CRS Winter Symposium, Salt Lake City, Utah, USA, February 21–24*, **2005**, 9.
[19] A. Harada, K. Kataoka, *Macromolecules* **1995**, *28*, 5294.

Received: December 21, 2005
Published online on ■■ ■■, 2006

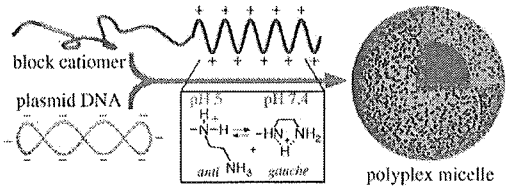

A polymer that delivers! A poly(ethylene glycol)-based block catiomer with an ethylenediamine unit as a side chain was prepared by an aminolysis reaction, and its utility as a gene carrier was investigated. This polymer provided efficient and less toxic transfection even toward primary cells.

N. Kanayama, S. Fukushima, N. Nishiyama, K. Itaka, W.-D. Jang, K. Miyata, Y. Yamasaki, U.-i. Chung, K. Kataoka**

■■ – ■■

A PEG-Based Biocompatible Block Catiomer with High Buffering Capacity for the Construction of Polyplex Micelles Showing Efficient Gene Transfer toward Primary Cells

NANO LETTERS
2005
Vol. 5, No. 12
2426−2431

Nanotechnology-Based Photodynamic Therapy for Neovascular Disease Using a Supramolecular Nanocarrier Loaded with a Dendritic Photosensitizer

Ryuichi Ideta,[†,‡] Fumitaka Tasaka,[†,‡,▽] Woo-Dong Jang,[†,§] Nobuhiro Nishiyama,[∥] Guo-Dong Zhang,[§] Atsushi Harada,[⊥] Yasuo Yanagi,[‡] Yasuhiro Tamaki,[‡] Takuzo Aida,[#] and Kazunori Kataoka*[,§,∥]

Department of Ophthalmology, Graduate School of Medicine, The University of Tokyo, 7-3-1 Hongo, Bunkyo-ku, Tokyo 113-8655, Japan, Department of Materials Science and Engineering, Graduate School of Engineering, The University of Tokyo, 7-3-1 Hongo, Bunkyo-ku, Tokyo 113-8656, Japan, Center for Disease Biology and Investigative Medicine, Graduate School of Medicine, The University of Tokyo, 7-3-1 Hongo, Bunkyo-ku, Tokyo 113-0033, Japan, Department of Applied Materials Science, Graduate School of Engineering, Osaka Prefecture University, 1-1 Gakuen-cho, Sakai, Osaka 599-8531, Japan, Department of Chemistry and Biotechnology, Graduate School of Engineering, The University of Tokyo, 7-3-1 Hongo, Bunkyo-ku, Tokyo 113-8656, Japan, and Research & Development Division, Santen Pharmaceutical Co., Ltd., 8916-16 Takayama-cho, Ikoma, Nara 630-0101, Japan

Received August 23, 2005; Revised Manuscript Received October 3, 2005

ABSTRACT

Photodynamic therapy (PDT) for exudative age-related macular degeneration (AMD) was evaluated using a supramolecular nanomedical device, that is, a novel dendritic photosensitizer (DP) encapsulated by a polymeric micelle formulation. The characteristic dendritic structure of the DP prevents aggregation of its core sensitizer, thereby inducing a highly effective photochemical reaction. With its highly selective accumulation on choroidal neovascularization (CNV) lesions, this treatment resulted in a remarkably efficacious CNV occlusion with minimal unfavorable phototoxicity.

Photodynamic therapy (PDT) is one of the noninvasive ways of treating malignant tumors or macular degeneration.[1] PDT is based on the delivery of a photosensitizer (PS) to the target tissue after the administration of PS. Photoirradiation by appropriate laser light generates highly reactive oxygen species, such as singlet oxygen, which results in the oxidative destruction of target tissue. There are several kinds of already developed PSs for the clinical evaluation of their photodynamic efficacy. Most of the conventional PSs have large π-conjugation domains to extend their absorption cross sections and basically have hydrophobic characteristics. Therefore, PSs form aggregates easily, which produce the self-quenching of the excited state, in aqueous medium because of their $\pi-\pi$ interaction and hydrophobic characteristics. To improve the photodynamic efficacy, the efficient delivery of PSs and high quantum yield of the singlet oxygen generation are significantly important. On the basis of this information, we have reported a dendrimer-based PS recently, dendrimer porphyrin (DP),[2−4] in which the focal porphyrin is surrounded by the third generation of poly(benzyl ether) dendrons (Figure 1a).[5] Unlike conventional PSs, the DP ensures the efficacy of singlet oxygen production even at an extremely high concentration because the dendritic

* Corresponding author. Address: Department of Materials Science and Engineering, Graduate School of Engineering, The University of Tokyo, 7-3-1 Hongo, Bunkyo-ku, Tokyo 113-8656, Japan. Fax +81-3-5841-7139. Tel +81-3-5841-7138. E-mail; kataoka@bmw.t.u-tokyo.ac.jp.
† Equally contributed to this work.
‡ Department of Ophthalmology, Graduate School of Medicine, The University of Tokyo.
§ Department of Materials Science and Engineering, Graduate School of Engineering, The University of Tokyo.
∥ Center for Disease Biology and Investigative Medicine, Graduate School of Medicine, The University of Tokyo.
⊥ Osaka Prefecture University.
Department of Chemistry and Biotechnology, Graduate School of Engineering, The University of Tokyo.
▽ Santen Pharmaceutical Co., Ltd.

10.1021/nl051679d CCC: $30.25
Published on Web 10/27/2005

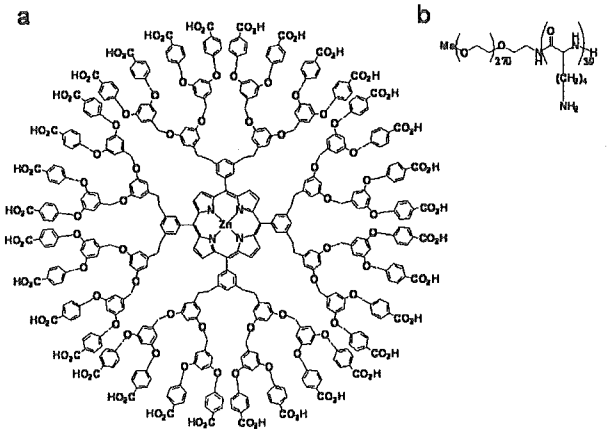

Figure 1. Structures of DP (a) and poly(ethylene glycol)-*block*-poly(L-lysine) (PEG-b-P(Lys) (b).

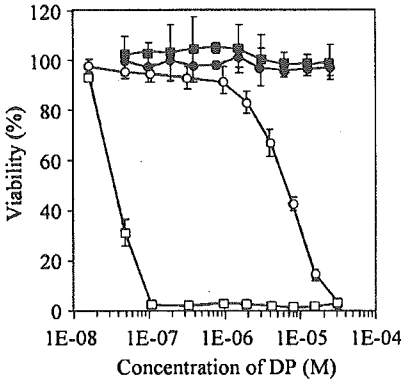

Figure 2. In vitro cytotoxicity of free DP (circle) and DP-loaded micelle (square) in the presence (open symbol) or absence (closed symbol) of photoirradiation. Encapsulation of DP into the micelle resulted in a 280-fold increase in the phototoxicity in vitro.

envelope of DP can prevent aggregation of the central porphyrin.[6] Also, the 32 negative charges on DP allow its stable incorporation into a supramolecular nanocarrier, the polyion complex (PIC) micelle,[7] through electrostatic interaction with oppositely charged block copolymers (Figure 1b).[8,9]

Alternatively, age-related macular degeneration (AMD), a condition caused by choroidal neovascularization (CNV), is a major cause of legal blindness in developed countries. Recently, large randomized control studies demonstrated that PDT with Visudyne, a liposomal formulation of verteporfin, prevents severe visual loss due to CNV and was approved for clinical use.[10,11] However, because of the intractableness of AMD, most patients require repeated treatments every three months, still suffering from a reduced quality of life.[12] It should also be noted that even with the repeated PDT treatment, most patients end in visual loss because of recurring CNV,[13] thus prompting investigators to search for alternative PSs with even higher PDT efficacies. For effective PDT against AMD, the selective delivery of PS to the CNV lesions and an effective photochemical reaction at the CNV sites is necessary. In regard to the delivery of PS, low-density lipoproteins and antibodies against endothelial cell markers have been used as carrier molecules;[14] however, PS also distributes to normal vessels to some extent because normal vessels also express such markers. In addition, as described previously, the increased loading of PSs to drug vehicles could change the photochemical reaction mechanism from type II to type I because of the formation of aggregates, leading to a diminished photodynamic efficacy.[15] Thus, there is a strong impetus to develop novel PS formulations from the standpoint of both the efficiency of the delivery and photochemical reactions of the PS itself. Herein, we report the first example of the in vivo evaluation of dendritic PS for PDT treatment against AMD and wish to highlight the selective accumulation and photodynamic effect of the DP-loaded micelle on the CNV lesions.

Before the in vivo experiment, the photoinduced cytotoxic property of DP and the DP-loaded micelle was evaluated against Lewis lung cells, where the DP-loaed micelle was prepared as follows. A negatively charged third-generation ionic DP having 32 carboxylate end groups and PEG-b-P(Lys) was prepared by a method reported previously.[8] The PEG-b-P(Lys) was dissolved in aqueous NaH_2PO_4 (10 mM, pH = 4.95) and added to an aqueous solution of DP in Na_2HPO_4/0.1 N NaOH (10 mM Na_2HPO_4, pH = 11.54) to give a solution (10 mM, pH = 7.30) containing DP-loaded micelles, in which the molar ratio of the carboxylate end groups and lysine residues was adjusted to unity. The prepared PIC micelle had a unimodal size distribution. As shown in Figure 2, neither the DP nor DP-loaded micelle exhibit any toxic profiles under a dark condition, whereas either the DP or DP-loaded micelle shows a strong cytotoxicity under light irradiation. Notably, the encapsulation of DP into the micelle resulted in a 280-fold increase in the phototoxicity.

In an attempt to deliver PS to the CNV sites, a free DP and a DP-loaded PIC micelle were examined. To investigate the accumulation of the DP-loaded micelles encapsulating DP in the CNV lesions, we created experimental CNV as follows.[16] A general anesthesia was induced with an intraperitoneal injection (1000 μL/kg) of a mixture (7:1) of ketamine hydrochloride (Ketalar, Sankyo, Tokyo, Japan) and xylazine hydrochloride (Celactal, Bayer, Tokyo, Japan) or by the inhalation of diethyl ether. The pupil was dilated with one drop of 0.5% tropicamide (Mydrin M, Santen Pharmaceutical, Osaka, Japan) for photocoagulation. Four laser photocoagulations were applied to each eye of 16 rats (Male Brown Norway (BN) rats, 60−80 g, Saitama Animal Lab., Inc., Saitama, Japan) between the major retinal vessels around the optic disk with a diode-laser photocoagulator (DC-3000®, NIDEK, Osaka, Japan) and a slit lamp delivery system (SL150, Topcon, Tokyo, Japan) at a spot size of 75 μm, duration of 0.05 s, and intensity of 300 mW. By tail vein injection, 400 μL of the DP-loaded micelle encapsulating 1.5 mg/mL DP or 400 μL of free DP (1.5 mg/mL) was administered into rats 7 days after the photocoagulation. After the rats were sacrificed with an overdose of sodium pentobarbital, the eyes were enucleated immediately and snap-frozen in OCT compound 0.25, 1, 4, and 24 h later for the

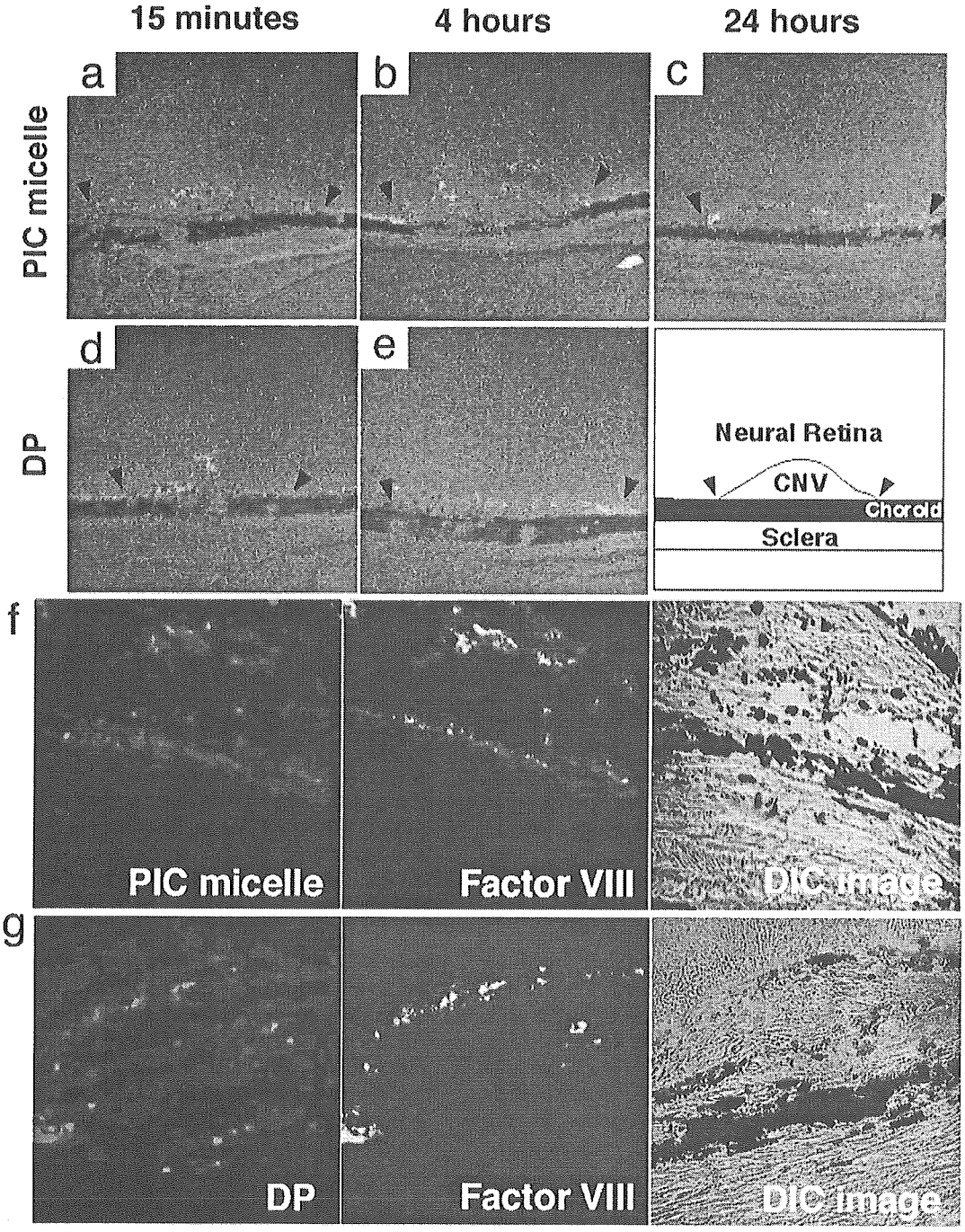

Figure 3. Accumulation of DP after administration of DP-loaded micelles to rats with experimental CNV (a–e). Accumulation of the DP-loaded micelle (a–c) and free DP (d and e) to experimental CNV. When the DP-loaded micelle was administered, the accumulation of DP in CNV lesions was observed as early as 15 min after the injection, peaked at 4 h, and was still evident 24 h after the injection. Whereas, after the free DP injection, DP was also present in CNV lesions for up to 4 h, but disappeared within 24 h (f and g). Immunohistochemistry shows the localization of the micelle and DP and factor VIII-positive endothelial cells. Note that DP is present within the factor VIII-positive endothelial cells when the DP-loaded micelle is administered, whereas DP was present mainly outside the factor VIII-positive endothelial cells when free DP was administered.

PIC micelle group (n = 4 at each time point) and 1 h later for the free DP group (n = 4). The frozen sections were mounted using the ProLong Antifade Kit (Molecular Probes, Eugene, Oregon) and observed under a fluorescent microscope (model IX, Olympus, Tokyo, Japan). Interestingly, the results showed an effective and selective accumulation of the micelle in the CNV lesions, indicating that the CNV lesions may have characteristic features similar to solid tumor vasculatures, such as hyperpermeability and impaired lymphatic drainage (i.e., so-called EPR effect[17]).[18–21] The

Table 1. CNV Closure Rate (%) after PDT

PDT condition	observation days	light fluence 0 J/cm^2	5 J/cm^2	50 J/cm^2
control	1	31.7 ± 13.4		
	7	15.0 ± 3.5		
treatment at 0.25 h	1	20.9 ± 4.2	19.4 ± 5.6	20.8 ± 4.2
after DP administration	7	25.0 ± 8.3	33.3 ± 8.3	18.8 ± 2.1
treatment at 0.25 h after	1	33.3 ± 0	77.7 ± 5.6	77.1 ± 2.9
DP-loaded micelle administration	7	25.0 ± 8.3	80.5 ± 2.8	83.4 ± 5.2
treatment at 4 h after DP-loaded	1	33.3 ± 0	60.0 ± 10.0	72.2 ± 15.5
micelle administration	7	25.0 ± 8.3	81.7 ± 1.7	77.8 ± 2.8

accumulation of DP in the CNV lesions was observed by histological analysis. For the histological analysis, prepared frozen sections were stained with FITC-conjugated monoclonal antibody against factor VIII (Dako cytomation, San Diego, CA), mounted with the ProLong Antifade Kit (Molecular Probes, Eugene, Oregon), and observed under a fluorescent microscope (model IX, Olympus, Tokyo, Japan). Both the free DP and DP-loaded micelles were recruited clearly in the CNV lesions (Figure 3a–e).

However, they exhibited drastically different aspects of accumulation. When the DP-loaded micelle was administered, the accumulation of DP to the CNV lesions was observed as early as 15 min after the injection, peaked at 4 h, and was still evident 24 h after the injection. Interestingly, the immunohistochemical analysis demonstrated that DP was present within the factor VIII-positive endothelial cells when the DP-loaded micelle was administered (Figure 3f). In contrast, after the free DP injection, DP concentrated in the CNV lesion up to 4 h (Figure 3d and e) but disappeared within 24 h. The immunohistochemical analysis demonstrated that DP was present not only in the factor VIII-positive endothelial cells but also outside of those cells when compared to the DP-loaded micelle administration (Figure 3g). These observations agree with our previous finding in vitro that the free DP exhibits a lowered cellular uptake because of its negatively charged periphery.[3] Therefore, the

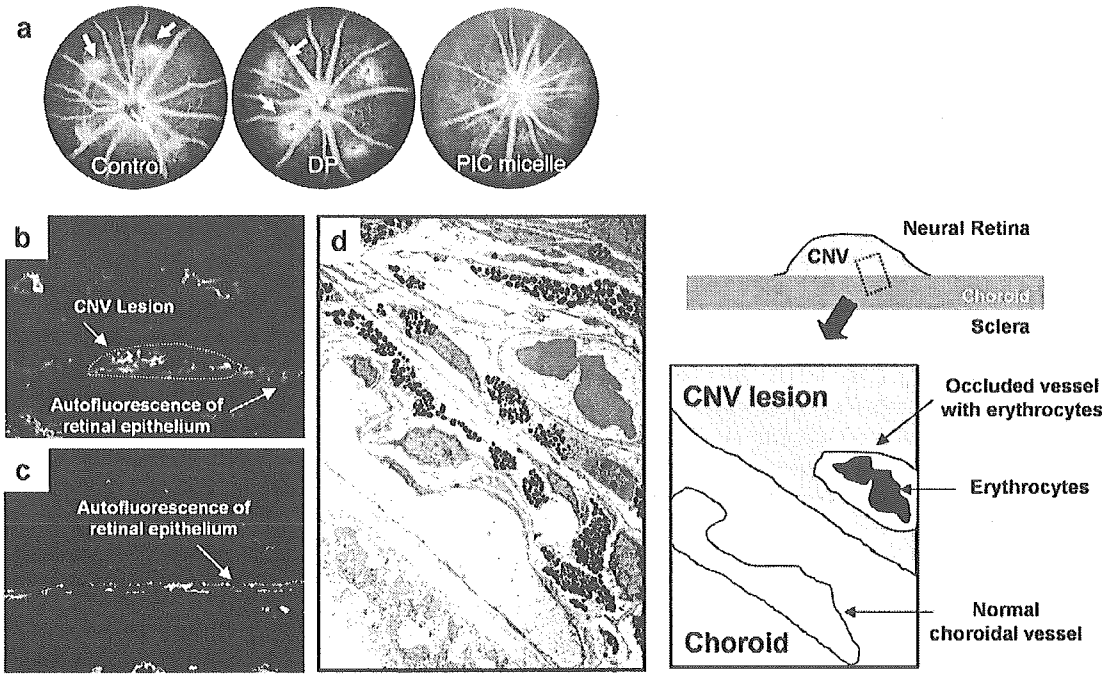

Figure 4. Efficacy of PDT laser after administration of the DP-loaded micelle. (a) Representative images of fluorescein angiograms in control, PDT-laser-irradiated eye after free DP was administered (DP), and PDT-laser-irradiated eye after the DP-loaded micelle was administered (PIC micelle). Note that the enhanced accumulation of DP-loaded micelles in CNV lesions resulted in a significantly pronounced photodynamic effect, whereas almost all of the CNV lesions showed a strong hyperfluorescence (marked with arrows), and the CNV endothelial cells appeared normal when free DP was administered. (b) Immunostaining of the endothelial cells with factor VIII antibody. Strong fluorescence from the CNV lesion is observable. (c) Immunostaining of the endothelial cells with factor VIII antibody after PDT treatment with DP-loaded micelle. Note that CNV lesion is occluded, and only autofluorescence from retinal pigment epithelium is observable. (d) Transmission electron microscopy of the CNV lesion of the PDT laser-irradiated eye after the DP-loaded micelle was administered. The neovascular blood vessel in CNV lesion is occluded by erythrocytes, whereas the normal choroidal vessel is not destroyed.

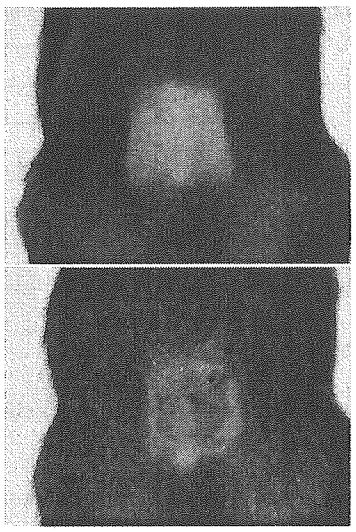

Figure 5. Macroscopic skin phototoxicity of DP-loaded micelle (top panel) and Photofrin (bottom panel). Skin phototoxicity was not observed macroscopically when the rats were exposed to broadband visible light 4 h after the injection of a DP-loaded micelle, whereas a severe phototoxicity was observed after the injection of Photofrin.

DP-loaded micelle is a very effective vehicle for delivery to factor VIII-positive endothelial cells for efficient photodynamic treatment.

Indeed, the enhanced accumulation of the micelle-encapsulated DP into CNV lesions resulted in a significantly pronounced photodynamic effect, which was evaluated using fluorescein angiography. When the PDT laser was applied 15 min after the injection of a DP-loaded micelle, 78% of the CNV lesions showed no fluorescein leakage at day 1 (Table 1). At day 7, the hypofluorescence persisted (Table 1), suggesting that leakage from the CNV lesions was still reduced. Similar results were observed when PDT was performed 4 h after the injection (Table 1). In sharp contrast, neither the administration of DP alone nor the application of the PDT laser alone affected the CNV activity (i.e., a similar proportion of the CNV lesions showed leakage (ca. 20−30% closure rate; Table 1, Figure 4a)).

Immunohistochemical analysis with factor-VIII demonstrated that CNV endothelial cells were destroyed by the PDT laser compared to the untreated control lesion when the lesion was treated with the laser after the administration of a DP-loaded micelle (Figure 4b and c). Transmission electron microscopy revealed that the vessels in the CNV lesion regressed to collagen tubes without endothelial cells or were occluded by erythrocytes (Figure 4d). Importantly, the endothelial cells of the overlying normal blood vessel in the retina and choroid in the treated lesions were not destroyed, even after the application of the PDT laser at maximum energy after the administration of the DP-loaded micelle, probably because neither the PIC micelle nor free DP was taken up into the endothelial cells in normal blood vessels. Moreover, as shown in Figure 5, skin phototoxicity is not macroscopically observable when the rats were exposed to broadband visible light (Xenon lamp equipped with a filter passing light of 377−700 nm, incident light irradiance; approximately 30 mW/cm^2) 4 h after the injection of the DP-loaded micelle (400 μL, 1.5 mg/mL), which is in sharp contrast to the results observed after the injection of a clinically used PS formulation, Photofrin (400 μL, 1.5 mg/mL). In contrast to the suppressive effect after the administration of the DP-loaded micelle, almost all of the CNV lesions showed a strong hyperfluorescence (i.e., no occlusion of CNV) and the CNV endothelial cells appeared normal when free DP was applied under identical PDT conditions (Figure 4a and Table 1). In addition, as described previously, the encapsulation of DP into the micelle resulted in a 280-fold increase in phototoxicity. Because the DP-loaded micelle is assumed to dissociate gradually into the constituent DP and block copolymer in the body by dilution, long-term phototoxicity is avoidable after PDT using this micelle.

In the present paper, a novel concept for the treatment of CNV using the combination of a dendrimer photosensitizer and polymeric micelles was presented. The DP-loaded micelle achieved a highly selective accumulation of DP in the CNV lesions, and a lower power energy of light was sufficient to occlude the CNV lesions. This might be attributed to the unique characteristic of DP; the aggregation of the core porphyrin is sterically prevented even at a remarkably high concentration. Our data suggest that the DP-loaded micelles enhanced the efficacy of PDT significantly while circumventing side effects to the normal retinal and choroidal vessels and skin. Also, this protocol is applicable to the PDT of solid tumors. From the standpoint of the clinical use for solid tumors, we are developing dendritic PSs with longer excitation wavelengths currently. Nevertheless, our results strongly suggest the usefulness of dendritic PSs and their micellar formulation for effective PDT. The data in this communication will provide a novel paradigm for practical use in biomedical fields as dendrimer-based nanomedicines.

Acknowledgment. This study was supported by Industrial Technology Research Grant Program in 2004 from New Energy and Industrial Technology Development Organization (NEDO) of Japan and partially supported by the Core Research for Evolutional Science and Technology (CREST) from the Japan Science and Technology Agency (JST).

References

(1) Pandey, R. K.; Zhang, G. *Porphyrin Handbook*; Kadish, K. M., Smith, K. M., Guilard, R., Eds.; Academic Press: San Diego, CA, 2000; Vol. 6.
(2) Tomioka, N.; Takasu, D.; Takahashi, T.; Aida, T. *Angew. Chem., Int. Ed.* **1998**, *37*, 1531.
(3) Jang, W.-D.; Nishiyama, N.; Zhang, G.-D.; Harada, A.; Jiang, D.-L.; Kawauchi, S.; Morimoto, Y.; Kikuchi, M.; Koyama, H.; Aida, T.; Kataoka, K. *Angew. Chem., Int. Ed.* **2005**, *44*, 419.
(4) Nishiyama, N.; Stapert, H. R.; Zhang, G.-D.; Takasu, D.; Jiang, D.-L.; Nagano, T.; Aida, T.; Kataoka, K. *Bioconjugate Chem.* **2003**, *14*, 58.
(5) Hawker, C. J.; Frechet, J. M. J. *J. Am. Chem. Soc.* **1990**, *112*, 7638.
(6) Sato, T.; Jiang, D.-L.; Aida, T. *J. Am. Chem. Soc.* **1999**, *121*, 10658.
(7) Harada, A.; Kataoka, K. *Science* **1999**, *283*, 65.
(8) Harada, A.; Kataoka, K. *Macromolecules* **1995**, *28*, 5294
(9) Stapert, H. R.; Nishiyama, N.; Jiang, D.-L.; Aida, T.; Kataoka, K. *Langmuir* **2000**, *16*, 8182.

(10) Bressler, N. M.; Arnold, J.; Benchaboune, M.; Blumenkranz, M. S.; Fish, G. E.; Gragoudas, E. S.; Lewis, H.; Schmidt-Erfurth, U.; Slakter, J. S.; Bressler, S. B.; Manos, K.; Hao, Y.; Haynes, L.; Koester, J.; Reaves, A.; Strong, H. A. *Arch. Ophthalmol.* **2002**, *120*, 1443.
(11) Ferris, F. L.; Fine, S. L.; Hyman, L. *Arch. Ophthalmol.* **1984**, *102*, 1640.
(12) Meads, C.; Hyde, C. *Br. J. Ophthalmol.* **2004**, *88*, 212.
(13) Wormald, R.; Evans, J.; Smeeth, L.; Henshaw, K. *Cochrane Database Syst. Rev.* **2003**, CD002030.
(14) Renno, R. Z.; Miller, J. W. *Adv. Drug Delivery Rev.* **2001**, *52*, 63.
(15) Grossweiner, L. I.; Patel, A. S.; Grossweiner, J. B. *Photochem. Photobiol.* **1982**, *36*, 159.
(16) Yanagi, Y. *Invest. Ophthalmol. Visual Sci.* **2003**, *44*, 751.
(17) Matsumura, Y.; Maeda, H. *Cancer Res.* **1986**, *46*, 6387.
(18) Nishiyama, N.; Okazaki, S.; Cabral, H.; Miyamoto, M.; Kato, Y.; Sugiyama, Y.; Nishio, K.; Matsumura, Y.; Kataoka, K. *Cancer Res.* **2003**, *63*, 8977.
(19) Kwon, G.; Suwa, S.; Yokoyam, M.; Okano, M.; Sakurai, Y.; Kataoka, K. *J. Controlled Release* **1994**, *29*, 17−23.
(20) Yokoyama, M.; Okano, T.; Sakuraj, Y.; Fukushima, S.; Okamoto, K.; Kataoka, K. *J. Drug Target.* **1999**, *7*, 171.
(21) Ideta, R.; Yanagi, Y.; Tamaki, Y.; Tasaka, F.; Harada, A.; Kataoka, K. *FEBS Lett.* **2004**, *557*, 21.
(22) Boas, U.; Heegaard, P. M. H. *Chem. Soc. Rev.* **2004**, *33*, 43.

NL051679D

Available online at www.sciencedirect.com

SCIENCE DIRECT

Journal of Controlled Release 109 (2005) 15–23

journal of controlled release

www.elsevier.com/locate/jconrel

Freeze-dried formulations for in vivo gene delivery of PEGylated polyplex micelles with disulfide crosslinked cores to the liver

Kanjiro Miyata [a,c], Yoshinori Kakizawa [a], Nobuhiro Nishiyama [b], Yuichi Yamasaki [a,c], Tsunamasa Watanabe [d], Michinori Kohara [d], Kazunori Kataoka [a,b,c,*]

[a] *Department of Materials Science and Engineering, Graduate School of Engineering, The University of Tokyo, 7-3-1 Hongo, Bunkyo-ku, Tokyo 113-8656, Japan*

[b] *Center for Disease Biology and Integrative Medicine, Graduate School of Medicine, The University of Tokyo, 7-3-1 Hongo, Bunkyo-ku, Tokyo, 113-0033, Japan*

[c] *CREST, Japan Science and Technology Agency, Japan*

[d] *The Tokyo Metropolitan Institute of Medical Science, 3-18-22 Honkomagome, Bunkyo-ku, Tokyo, 113-8613, Japan*

Received 1 March 2005; accepted 15 August 2005

Abstract

A stable, freeze-dried formulation consisting of a core-shell-type polyplex with a poly(ethylene glycol) (PEG) shell (polyplex micelles) was prepared from a polyion complex of plasmid DNA (pDNA) and thiolated PEG-poly(L-lysine) block copolymers. The use of lyoprotectants was avoided by crosslinking the core with disulfide bonds. The crosslinked polyplex micelles (CPMs) showed excellent stability during freeze-drying and reconstitution processes, which is in sharp contrast with the formation of visible agglomerates from the non-crosslinked polyplex micelles (NCPMs) after a similar process. A thiolation degree higher than 13% of the lysine residues was required to achieve sufficient tolerability of the CPMs during the freeze-drying/reconstitution cycle. Dynamic light scattering measurements and atomic force microscopy observations demonstrated that the original size and shape of the CPMs with a thiolation degree of higher than 13% were maintained even after the freeze-drying. Furthermore, the CPMs reconstituted from the freeze-dried state achieved a transfection efficiency as high as that of the original samples. The intravenous injection of the CPM with a thiolation degree of 37% into mice via the orbital vein led to an appreciably uniform gene expression of a yellow fluorescence protein variant (Venus) in the liver, while no gene expression was observed in the case of the free pDNA injection. The procedure of disulfide crosslinking of the polyplex micell core allows the preparation of non-viral gene vectors as a powder formulation without the use of any lyoprotectants. This achievement is certainly useful for pharmaceutical applications and exhibits many advantages, including easy concentration adjustments of dosing samples, long-term storage stability, and large-scale production reproducibility.

* Corresponding author. Department of Materials Engineering, Graduate School of Engineering, The University of Tokyo, 7-3-1 Hongo, Bunkyo-ku, Tokyo 113-8656, Japan. Tel. +81 3 5841 7138; fax: +81 3 5841 7139.
E-mail address: kataoka@bmw.t.u-tokyo.ac.jp (K. Kataoka).

0168-3659/$ - see front matter © 2005 Elsevier B.V. All rights reserved.
doi:10.1016/j.jconrel.2005.09.043

1. Introduction

Non-viral vector systems based on synthetic cationic lipids and polymers are attractive alternatives to viral vector systems in gene therapy, because of the low immunogenicity, the ease of manufacturing, and further, the possibility of structural design with various intelligent functions designed to improve transfection [1–3]. Nevertheless, substantial issues must still be resolved before non-viral vectors can become practical formulations with clinical utility. One of these issues from a pharmaceutical viewpoint is the inadequate stability of non-viral vectors, i.e., many of them have low colloidal stability in aqueous solutions, resulting in the formation of insoluble aggregates. Accordingly, the long-term storage of the vector systems presents crucial difficulties. A powder formulation of non-viral vectors, which can be reconstituted to a colloidal dispersion by simply adding water or a buffer, is exceedingly useful in in vivo applications, for large scale preparation of the product, as well as for simple concentration adjustments to the dosing sample.

In general, reconstitution of the freeze-dried polyplex and lipoplex formulations results in the formation of micron-sized aggregates, and consequently, their transfection efficiency undergoes a substantial decrease. To avoid such aggregation, several approaches have been considered so far. For example, the addition of an excess of saccharide, e.g., sucrose, as a lyoprotectant may prevent the formulation from aggregation accompanying freeze-drying [4–7]. An alternative approach involves the covalent attachment of hydrophilic poly(ethylene glycol) (PEG) segments onto the DNA complexes as a steric barrier [8–11]. This method of PEGylation is especially useful for in vivo applications, because dose adjustment does not require the consideration of any additive concentration. Nevertheless, even with this approach, simple PEGylation may not be sufficient to completely prevent aggregation of the complexes [9,10]. Recently, a novel type of PEGylated polyplex, called polyplex micelles, has been developed by our group through the complexation of plasmid DNA (pDNA) and PEG-poly(L-lysine) block copolymers (PEG-PLL) [12–15]. Disulfide crosslinking was introduced into the micelle core to stabilize the structure in an extracellular entity, while facilitating smooth release of the entrapped pDNA in an intracellular reductive environment [16–18]. Note that the intracellular compartment has a 50~1000 times higher glutathione concentration than the extracellular milieu [19]. Here, we wish to report that these disulfide-crosslinked polyplex micelles (CPMs) have a pharmaceutical advantage of considerable stability during the freeze-drying process, exhibiting nearly identical dispersion characteristics, as well as transfection efficiencies, as the initial formulation even after reconstitution. The densities of disulfide crosslinking were optimized so as to reveal an appreciable transfection capacity, both in in vitro transfection experiments with cultured cell lines and in in vivo intravenous transfection studies of the liver.

2. Materials and methods

2.1. Reagents

α-Methoxy-ω-amino-poly(ethylene glycol) (M_w= 12,000) was purchased from Nippon Oil and Fats Co., Ltd. (Tokyo, Japan). The PEG-PLL block copolymers with an average polymerization degree of the PLL segment of 71 was synthesized as previously reported [12]. *N*-succinimidyl 3-(2-pyridyldithio)propionate (SPDP) and dithiothreitol (DTT) were purchased from Wako Pure Chemical Co., Ltd. (Osaka, Japan). *N*-methyl-2-pyrrolidone (NMP) was purchased from Aldrich Co., Inc. (Milwaukee, USA). A pGL3 control vector, which was purchased from Promega Co., Inc. (Madison, USA), was used for the physicochemical characterization. A plasmid vector coding for luciferase with a CAG promoter provided by RIKEN, Japan, was used in the in vitro transfection experiment (luciferase assay) [20]. A plasmid vector coding for a yellow fluorescence protein variant with the mutation F46L (Venus), which exhibits enhanced and stable fluorescence under intracellular conditions, was provided by Dr A. Miyawaki, RIKEN, Japan, and used for the in vivo gene delivery experiments [21]. The pDNAs were amplified in competent DH5α *Escherichia coli* and purified using a HiSpeed Plasmid Maxi Kit purchased from QIAGEN Sciences Co., Inc. (Germantown, MD). A Micro BCA™ Protein Assay Reagent Kit was purchased from PIERCE Co., Inc. (Rockford, USA).

2.2. Synthesis of thiolated PEG-PLL

Introduction of the 3-(2-pyridyldithio)propionyl moiety into the flanking amino groups of the PLL segment of PEG-PLL was performed as previously reported [18]. Typically, PEG-PLL (51 mg) and SPDP (25 mg) were dissolved in *N*-methylpyrrolidone (4.5 ml) containing 5 wt.% LiCl, and the mixture was stirred at 20 °C for 24 h after the addition of a 10% volume of *N,N*-diisopropylethylamine. The sample solution was purified by precipitation into an approximately 20-times-excess volume of diethyl ether. The precipitated polymer was redissolved in 0.01 N HCl (20 ml), dialyzed against distilled water, and lyophilized to obtain the final product (45 mg). The degree of thiol substitution for each thiolated PEG-PLL was determined from the peak intensity ratio of the methylene protons of PEG (OCH_2CH_2, δ=3.5 ppm) to the pyridyl protons of the 3-(2-pyridyldithio)propionyl group (C_5H_4N, δ=7.2–8.3 ppm) in the ^1H NMR spectrum (D_2O, 25 °C). In this study, thiolated PEG-PLLs with thiol substitution degrees of 5%, 13%, 28% and 37% were synthesized and used to prepare the CPMs, abbreviated as CPM-5, -13, -28, and -37, respectively.

2.3. Preparation of non-crosslinked and crosslinked polyplex micelles

Each polyplex micelle was prepared by the following procedure: A non-crosslinked polyplex micelle (NCPM) was obtained by simply mixing PEG-PLL (2 mg/ml) and pDNA (50 μg/ml) solutions in 10 mM Tris–HCl buffer (pH 7.4) at a *N/P* ratio of 2. Here, the *N/P* ratio was defined as the residual molar ratio of lysine units in the PEG-PLL to phosphate units in the pDNA. The pDNA concentration in the final solution was adjusted to 33.3 μg/ml. These samples were subjected to the following experiments after an overnight incubation at ambient temperature. To prepare the CPMs, a 10 mM Tris–HCl (pH 7.4) solution of thiolated PEG-PLL (1–2 mg/ml) was mixed with a 10% volume of 100 mM DTT in the same buffer to reduce the 3-(2-pyridyldithio)propionyl group to a thiol group. After 30 min at ambient temperature, the polymer solution with DTT was mixed with the pDNA solution (50 μg/ml) in 10 mM Tris–HCl (pH 7.4) to form the polyplex micelle at a *N/P* ratio of 2. Note that the *N/P* ratio in the thiolated systems was defined as the residual molar ratio of non-thiolated lysine units in the thiolated PEG-PLL to phosphate units in pDNA. After an overnight incubation period at ambient temperature, the thiolated polyplex micelle solution was dialyzed against 10 mM Tris–HCl (pH 7.4) containing 0.5% dimethylsulfoxide at 37 °C for 24 h, followed by an additional 2 days of dialysis for the removal of dimethylsulfoxide. During these dialysis processes, the thiol groups of thiolated PEG-PLL in the micelles were oxidized to form the disulfide crosslinks. The remaining thiol groups in the crosslinked polyplex micelles were determined by Ellman's method to be less than 10% of the initial value [22]. The prepared polyplex micelles were stored at 4 °C for 1 week, verifying that no precipitate formation occurred, and were subjected to the freeze-drying study.

2.4. Freeze-drying and reconstitution of polyplex micelles

Polyplex micelles with a pDNA concentration of 33.3 μg/ml in 10 mM Tris–HCl (pH 7.4) buffer were freeze-dried in 1–1.5 ml aliquots. The sample solutions were filled in 5 ml glass vacuum vials with rubber freeze-drying stoppers and plunged into liquid nitrogen for at least 3 min. The frozen samples were immediately freeze-dried using a freeze-dryer FD-5N (EYELA, Tokyo, Japan). After overnight lyophilization, the samples were reconstituted with distilled water and incubated overnight at ambient temperature.

2.5. UV measurements

To determine the amount of pDNA in the solution after reconstitution of the freeze-dried samples, the absorbance at 260 nm was measured using a V-550 instrument (JASCO, Tokyo, Japan). The pDNA concentration in the supernatant of the polyplex solutions was calculated as the percentage ratio of A_{260} of the samples before and after freeze-drying.

2.6. Dynamic light scattering measurements

Dynamic light scattering (DLS) measurements were carried out using a DLS-7000 instrument

(Otsuka Electronics Co, Ltd., Hirakata, Japan) to estimate the hydrodynamic diameters of polyplex micelles before and after freeze-drying. An Ar ion laser (λ=488 nm) was used as an incident beam. All the polyplex micelles were adjusted to a concentration of 33.3 μg pDNA/ml. The data obtained at a detection angle of 90° and a temperature of 25 °C were analyzed by a cumulant method to obtain the hydrodynamic diameters and polydispersity indices (μ/Γ^2).

2.7. Atomic force (AFM) imaging

AFM imaging of the CPMs was done by depositing 4 μl of each sample solution onto a freshly cleaved mica substrate and allowing to stand for 30 s. The solution was dried under a gentle flow of nitrogen gas. AFM imaging was performed in the tapping mode with standard silicon probes (160 μm in length, Olympus, Tokyo, Japan) on an NVB100 microscope (Olympus) controlled by the operating software of Nanoscope IIIa (Digital Instruments, Santa Barbara, CA, USA). The cantilever oscillation frequency was tuned to a cantilever resonance frequency of 260–340 kHz. The 256 × 256 images were recorded at a 0.5–2 μm/s linear scanning speed at a sampling density of 4–60 nm^2 per pixel. Raw AFM images were processed only for background removal (flattening) using the microscope manufacturer's image-processing software.

2.8. Dye exclusion assay

Polyplex micelle solutions were diluted with Tris–HCl (pH 7.4) buffer containing ethidium bromide (EtBr) to a concentration of 10 μg pDNA/ml and 2.5 μg EtBr/ml. The sample solutions were incubated at ambient temperature overnight. Fluorescence intensity of the samples at 590 nm with excitation at 510 nm was measured at 25 °C using a spectrofluorometer (FP-6500, JASCO, Tokyo, Japan).

2.9. In vitro transfection (Luciferase Assay)

293T cells were plated on 24-well culture plates. After a 24 h incubation period in 400 μl of Dulbecco's modified eagle medium (DMEM) containing 10% serum, the medium was replaced with 400 μl of transfection medium containing 10% serum. Thirty microliters of the polyplex micelle solution (33.3 μg pDNA/ml) were then applied to each well for transfection. After 24 h of incubation, the medium was replaced with 400 μl of the medium containing 10% serum, followed by an additional 24 h incubation. The cells were washed with 400 μl of Dulbecco's PBS, followed by the addition of 100 μl of cell culture lysis buffer (Promega). The luciferase assay was carried out using the Luciferase Assay System Kit (Promega), and the intensity of photoluminescence was measured by a Mithras LB 940 (Berthold technologies). The amount of protein in each well was concomitantly determined using the Micro BCA™ Protein Assay Reagent Kit.

2.10. In vivo gene expression of crosslinked polyplex micelles

The pDNA coding for the reporter gene, Venus, was used in in vivo experiments. Two hundred microliter of CPM-37 solution with a concentration of 585 μg pDNA/ml were injected into BALB/c mice (8–12 weeks, 20–21 g) via the orbital vein at ambient temperature, and their livers were then excised at a pre-defined time. The excised livers were stored at −80 °C after treatment with an OCT compound (Tissue-Tek, Sakura Finetek) as a low-temperature embedding medium. The liver samples were sliced using a cryostat, LEICA CM 3050S, and placed on an aminosilane-coated MicroSLIDEglass (Matsunami). The slices were washed three times with PBS and mounted with Permafluor aqueous mounting medium (Immunotech) containing 10 μM TO-PRO-3, a nucleus marker (Molecular Probe). After an incubation period of 15 min in the dark at ambient temperature, the samples were stored at 4 °C. Using a fluorescence microscope, Zeiss Axio Vision 3.1, the fluorescence emissions of Venus (528 nm) and TO-PRO-3 (661 nm) in the liver samples was observed using excitation wavelengths of 515 and 642 nm, respectively.

3. Results and discussion

3.1. Solubility of the polyplex micelles after freeze-drying

A solution of NCPM as a non-crosslinked control was freeze-dried from 10 mM Tris–HCl (pH 7.4)

buffer and then redissolved in distilled water. The freeze-drying process was carried out overnight for 1–1.5 ml of the polyplex solution with 33.3 μg pDNA/ml. Although the initial polyplex solution was clear without any visible precipitates, fibrous flocculates were observed after the freeze-drying and reconstitution processes. The pDNA concentration in the supernatant of the reconstituted NCPM solution was determined from the absorbance at 260 nm. A drastic decrease in the pDNA concentration was observed after reconstitution. Obviously, the NCPM underwent agglomeration in the course of freeze-drying, due to the poor solubility of the reconstituted samples.

Core-crosslinking of the micelles was then carried out as described in the Materials and methods section to prevent the agglomeration caused by freeze-drying. The core crosslinked polyplex micelles (CPMs) were freeze-dried from 10 mM Tris–HCl (pH 7.4) buffer and reconstituted in distilled water, followed by measurement of their absorbance at 260 nm. As shown in Fig. 1, the CPMs with a thiolation degree higher than 13% exhibited the same absorbance after freeze-drying as the initial CPM suspension, while the CPM with a lower thiolation degree of 5% underwent a substantial decrease in absorbance, similar to that seen with the NCPM. Obviously, a critical degree of crosslinking in the region of about 10% exists to prevent the agglomeration accompanying freeze-drying.

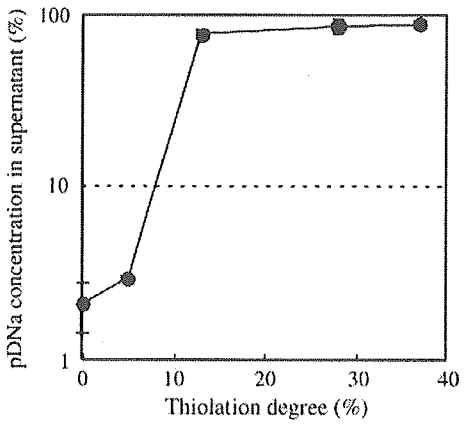

Fig. 1. The concentration of plasmid DNA in the supernatant of the polyplex micelle solutions after the freeze-drying and reconstitution processes. The pDNA concentration in the supernatant was determined from the absorbance at 260 nm. Data are given as mean ± standard deviation of triplicate samples.

3.2. Effect of freeze-drying on the size and morphology of polyplex micelles

The freeze-drying process generally induces an increase in the size of reconstituted polyplexes, hampering their biological activities. To evaluate the effect of crosslinking on the size of the polyplex micelles after freeze-drying, the hydrodynamic diameter was measured by DLS. The results shown in Fig. 2 (a) and (b) clearly reveal that CPM-13, -28, and -37, the samples showing favorable dispersion characteristics in the reconstituted solutions, retained their initial size and polydispersity (μ/Γ^2) even after the freeze-drying process. Note that these CPMs with a thiolation degree higher than 13% showed no change in the light scattering intensity after freeze-drying, whereas the intensity of the CPM-5 with a lower substitution degree significantly decreased to one-tenth of the initial value (data not shown). These results quantitatively indicate that a certain degree of core-crosslinking effectively prevents polyplex micelle agglomeration caused by freeze-drying.

Although the light scattering study provides the average size and distribution of the micelle population, information on the individual micelle, such as its morphology, is still ambiguous. Previous studies have suggested that structural alterations other than changes in the average particle size may have a definite effect on the biological activity [7]. Accordingly, the morphology of the individual CPM before and after the freeze-drying process was observed using AFM. The observation was carried out for dried samples on a freshly split mica disk. Fig. 3 clearly shows that the freeze-drying process caused a negligible change in the morphology of the CPM-28 micelles; similar toroidal and rod-like structures with a size of around 100 nm were observed in both AFM images of CPM-28 before (a) and after (b) freeze-drying. Also, the fluorescence intensity values of the samples in the buffer containing EtBr were the same both before and after freeze-drying CPMs with a thiolation degree higher than 13% (data not shown). These results strongly suggest that any structural changes caused by the

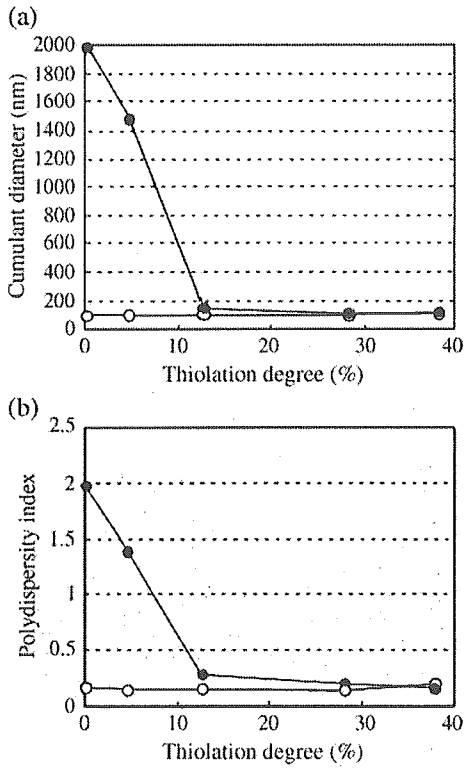

Fig. 2. (a) Cumulant diameters and (b) polydispersity indices (μ/Γ^2) of polyplex micelles before and after the freeze-drying process. The symbols, ○ and ●, stand for the values before and after freeze-drying, respectively.

freeze-drying process are negligible in the CPM systems with a thiolation degree higher than 13%. The excellent stability of the CPMs during freeze-drying may be due to the restricted motion of polymer components in the crosslinked core, which may protect the micelle from stress generated during the freeze-drying process. It should be noted that the PEG chain has a high flexibility, as characterized by a low Tg, yet, in turn, it demonstrates a high crystallization capability due to the short and simple repeating units in the strands. Eventually, micro-brownian motion of the PEG moiety during freeze-drying above the Tg may facilitate the rearrangement of PEG strands causing crystallization, resulting in increasing disorder of the micelle structure unless crosslinking was introduced into the core. It is worth mentioning that the CPM does not require any lyoprotectants for freeze-drying, which is certainly an advantage for the adjustment of the concentration and the amount of dosing samples in both in vitro and in vivo applications.

3.3. In vitro transfection efficiency

The effect of disulfide crosslinking on the transfection efficiency of the polyplex micelles was evaluated by in vitro transfection of the luciferase gene in cultured 293T cells. The cells were incubated with each polyplex micelle formulation in medium containing 10% FBS for 24 h, followed by an additional 24 h incubation period in the same medium

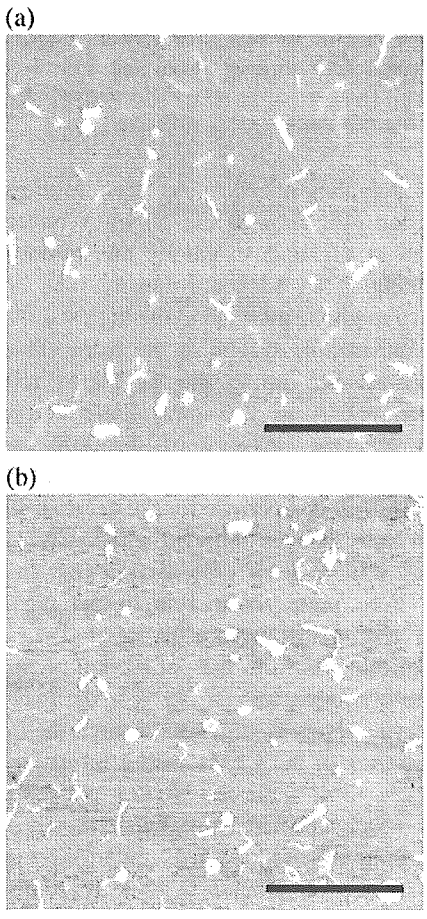

Fig. 3. AFM images of CPM-28. The panels (a) and (b) represent the samples before and after freeze-drying, respectively. The scale bars are equivalent to 1 μm. The data are presented using the height mode in the operating software of Nanoscope IIIa.

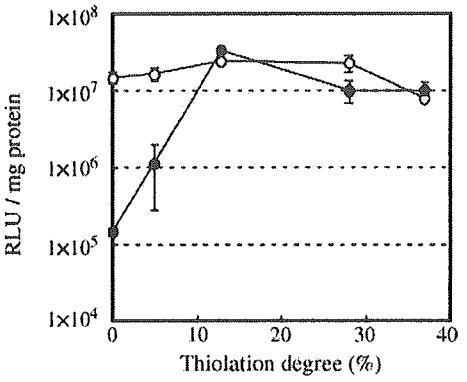

Fig. 4. Effect of freeze-drying and reconstitution processes on the in vitro transfection efficiency of CPM with different thiolation degrees. 293T cells were incubated with polyplex micelles in medium containing 10% serum for 24 h, followed by an additional incubation for 24 h. The symbols, ○ and ●, stand for the transfection efficiency before and after freeze-drying, respectively. Data are given as mean ± standard deviation of triplicate experiments.

without polyplex micelles. As seen in Fig. 4, the transfection efficiency of the polyplex micelles was enhanced to a certain extent by the introduction of crosslinking at an adequate density. The enhanced efficiency might be ascribed to the high stability of the crosslinked micelle system in the extracellular environment, as well as to the facilitated release of entrapped pDNA in the intracellular compartment through efficient cleavage of disulfide crosslinks introduced into the poly(L-lysine) segment; an attribute which may compensate for the decrease in charge density. Note that, as reported previously [18], the enhanced efficiency of CPMs compared to NCPM became even more remarkable in the presence of hydroxychloroquine, presumably due to the enhanced escape of micelles from the endosomal compartment [23]. Worth emphasizing in Fig. 4 is the fact that the freeze-drying process did not hamper the transfection efficiency of the CPMs with a thiolation degree higher than 13%, while the NCPM and the CPM-5, both of which underwent agglomeration during the freeze-drying process, showed a significant decrease in the transfection efficiency after freeze-drying. A similar tendency was also confirmed for Huh-7 cells (data not shown). These results are consistent with the physicochemical characterization of the polyplex micelles; the systems which retained their initial size and morphology even after the freeze-dry/reconstitution processes exhibited appreciable transfection efficiencies.

3.4. In vivo gene expression by CPM

In vivo gene expression of CPM-37, the formulation which showed an excellent stability during freeze-drying, was evaluated using a yellow fluo-

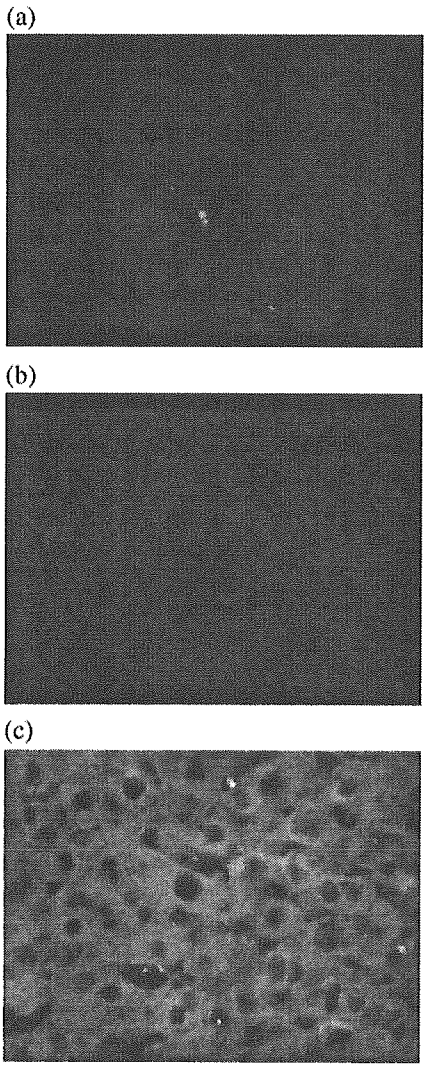

Fig. 5. Venus gene expression in mice liver after i.v. injection of CPM-37. The panels, (a), (b), and (c), represent the expression at 1, 3, and 5 days, respectively, after the injection of CPM-37 (585 μg pDNA/ml, 200 μl) through the orbital vein.

rescence protein with the mutation F46L (Venus) in the liver. The CPM-37 formulation was injected intravenously through the orbital vein of mice, and the liver was removed at a pre-defined time. The extracted livers were processed into thin-sectioned slices as described in the Materials and methods section, followed by observation under a fluorescence microscope. No transfection was confirmed for the i.v. injection of 200 μl of the naked pDNA solution with a concentration of 1000 μg pDNA/ml. On the other hand, definite expression of the Venus gene was exhibited with CPM-37 (585 μg pDNA/ml, 200 μl), as shown in Fig. 5 (a)–(c). Although no gene expression was detected until 3 days, almost all the hepatocytes in the thin-section expressed the Venus gene 5 days after the injection, presumably due to the time required for the cumulative amount of expressed Venus to reach the level detectable by fluorescence microscopy. Considering future therapeutic applications for liver diseases, a uniform transfection to the hepatocytes by CPMs is exciting.

4. Conclusion

Major concerns of pDNA complexes (lipoplexes and polyplexes) and their applicability as non-viral gene vectors involve the stability during long-term storage, as well as their dispersion behavior after reconstitution from a freeze-dried formulation. The regulated introduction of disulfide crosslinks into the core of polyplex micelles is a useful approach to formulate freeze-dried pDNA complexes stable during long-term storage with favorable dispersion upon reconstitution. Indeed, the CPMs with a thiolation degree higher than 13% retained their initial size, shape, and transfection efficiency, even after the freeze-dry/reconstitution processes. Moreover, the CPM showed uniform gene expression in the liver parenchymal cells after intravenous injection via the orbital vein in mice, demonstrating their utility in in vivo gene delivery via an intravenous route. In conclusion, the CPM system developed here for in vivo gene delivery has a wide utility as a practical formulation satisfying the requirements of easy concentration adjustments of dosing samples stability during long-term storage, and large-scale production reproducibility.

Acknowledgments

This work was financially supported by the Core Research Program for Evolutional Science and Technology (CREST) from the Japan Science and Technology Corporation (JST), as well as by Special Coordination Funds for Promoting Science and Technology from the Ministry of Education, Culture, Sports, Science and Technology of Japan (MEXT). The authors express their appreciation to Dr A. Miyawaki, RIKEN, Japan, and Dr H. Hamada, Sapporo Medical University, Japan, for providing the plasmid DNA.

References

[1] D. Luo, W.M. Saltzman, Synthetic DNA delivery systems, Nat. Biotechnol. 18 (2000) 33–37.
[2] T. Merdan, J. Kopecek, T. Kissel, Prospects for cationic polymers in gene and oligonucleotide therapy against cancer, Adv. Drug Deliv. Rev. 54 (2002) 715–758.
[3] Y. Kakizawa, K. Kataoka, Block copolymer micelles for delivery of gene and related compounds, Adv. Drug Deliv. Rev. 54 (2002) 203–222.
[4] J.Y. Cherng, P. Wetering, H. Talsma, D.J.A. Crommelin, W.E. Hennink, Freeze-drying of poly((2-dimethylamino)ethyl methacrylate)-based gene delivery systems, Pharm. Res. 14 (1997) 1838–1841.
[5] H. Talsma, J.Y. Cherng, H. Lehrmann, M. Kursa, M. Ogris, W.E. Hennink, M. Cotton, E. Wagner, Stabilization of gene delivery systems by freeze-drying, Int. J. Pharm. 157 (1997) 233–238.
[6] T.J. Anchordoquy, J.F. Carpenter, D.J. Kroll, Maintenance of transfection rates and physical characterization of lipid/DNA complexes after freeze-drying and reconstitution, Arch. Biochem. Biophys. 348 (1997) 199–206.
[7] M.dC. Molina, S.D. Allison, T.J. Anchordoquy, Maintenance of nonviral vector particle size during the freeze step of the lyophilization process is insufficient for preservation of activity: insight from other structural indicators, J. Pharm. Sci. 90 (2001) 1445–1455.
[8] K.Y. Kwok, R.C. Adami, K.C. Hester, Y. Park, S. Thomas, K.G. Rice, Strategies for maintaining the particle size of peptide DNA condensates following freeze-drying, Int. J. Pharm. 203 (2000) 81–88.
[9] T.K.C. Armstrong, L.G. Girouard, T.J. Anchordoquy, Effects of PEGylation on the preservation of cationic lipid/DNA complexes during freeze-thawing and lyophilization, J. Pharm. Sci. 91 (2002) 2549–2558.
[10] M. Kursa, G.F. Walker, V. Roessler, M. Ogris, W. Roedl, R. Kircheis, E. Wagner, Novel shielded transferrin-polyethylene glycol-polyethylenimine/DNA complexes for systemic tumor-targeted gene transfer, Bioconjug. Chem. 14 (2003) 222–231.

[11] M. Ganguli, K.N. Jayachandran, S. Maiti, Nanoparticles from cationic copolymer and DNA that are soluble and stable in common organic solvents, J. Am. Chem. Soc. 126 (2004) 26–27.
[12] S. Katayose, K. Kataoka, Water-soluble polyion complex associates of DNA and poly(ethylene glycol)-poly(L-lysine) block copolymer, Bioconjug. Chem. 8 (1997) 702–707.
[13] K. Itaka, A. Harada, K. Nakamura, H. Kawaguchi, K. Kataoka, Evaluation by fluorescence resonance energy transfer of the stability of nonviral gene delivery vectors under physiological conditions, Biomacromolecules 3 (2002) 841–845.
[14] M. Harada-Shiba, K. Yamauchi, A. Harada, I. Takamisawa, K. Shimokado, K. Kataoka, Polyion complex micelles as a vector for gene therapy—pharmacokinetics and in vivo gene transfer, Gene Ther. 9 (2002) 407–414.
[15] K. Itaka, K. Yamauchi, A. Harada, K. Nakamura, H. Kawaguchi, K. Kataoka, Polyion complex micelles from plasmid DNA and poly(ethylene glycol)-poly(L-Lysine) block copolymer as serum-tolerable polyplex system: physicochemical properties of micelles relevant to gene transfection efficiency, Biomaterials 24 (2003) 4495–4506.
[16] Y. Kakizawa, A. Harada, K. Kataoka, Environment-sensitive stabilization of core-shell structured polyion complex micelle by reversible cross-linking of the core through disulfide bond, J. Am. Chem. Soc. 121 (1999) 11247–11248.
[17] Y. Kakizawa, A. Harada, K. Kataoka, Glutathione-sensitive stabilization of block copolymer micelles composed of antisense DNA and thiolated poly(ethylene glycol)-block-poly(L-lysine): a potential carrier for systemic delivery of antisense DNA, Biomacromolecules 2 (2001) 491–497.
[18] K. Miyata, Y. Kakizawa, N. Nishiyama, A. Harada, Y. Yamasaki, H. Koyama, K. Kataoka, Block catiomer polyplexes with regulated densities of charge and disulfide cross-linking directed to enhance gene expression, J. Am. Chem. Soc. 126 (2004) 2355–2361.
[19] A. Meister, M.E. Anderson, Glutathione, Annu. Rev. Biochem 52 (1983) 711–760.
[20] H. Niwa, K. Yamamura, J. Miyazaki, Efficient selection for high-expression transfectants with a novel eukaryotic vector, Gene 108 (1991) 193–199.
[21] T. Nagai, K. Ibata, E.S. Park, M. Kubota, K. Mikoshiba, A. Miyawaki, A variant of yellow fluorescent protein with fast and efficient maturation for cell-biological applications, Nat. Biotechnol. 20 (2002) 87–90.
[22] P.W. Riddles, R.L. Blakeley, B. Zerner, Ellmans reagent—5,5′-dithiobis(2-nitrobenzoic acid)-re-examination, Anal. Biochem. 94 (1979) 75–81.
[23] K. Itaka, K. Miyata, A. Harada, H. Kawaguchi, K. Nakamura, K. Kataoka, Carrier-based drug delivery, in: S. Svenson (Ed.), ACS Symposium Series, vol. 879, ACS, Washington, D.C., 2004, pp. 154–160.

Light-induced gene transfer from packaged DNA enveloped in a dendrimeric photosensitizer

NOBUHIRO NISHIYAMA[1]*, AYA IRIYAMA[2]*, WOO-DONG JANG[3], KANJIRO MIYATA[3], KEIJI ITAKA[1], YUJI INOUE[2], HIDENORI TAKAHASHI[2], YASUO YANAGI[2], YASUHIRO TAMAKI[2], HIROYUKI KOYAMA[4] AND KAZUNORI KATAOKA[1,3†]

[1]Center for Disease Biology and Integrative Medicine, Graduate School of Medicine, The University of Tokyo, 7-3-1 Hongo, Bunkyo-ku, Tokyo 113-0033, Japan
[2]Department of Ophthalmology, University of Tokyo Hospital, 7-3-1 Hongo, Bunkyo-ku, Tokyo 113-8655, Japan
[3]Department of Materials Engineering, Graduate School of Engineering, The University of Tokyo, 7-3-1 Hongo, Bunkyo-ku, Tokyo 113-8656, Japan
[4]Department of Clinical Vascular Regeneration, The University of Tokyo Hospital, 7-3-1 Hongo, Bunkyo-ku, Tokyo 113-8655, Japan
*These authors contributed equally to this paper
†e-mail: kataoka@bmw.t.u-tokyo.ac.jp

Published online: 20 November 2005; doi:10.1038/nmat1524

The control of gene transfection in the body is a core issue in gene therapy. Photochemical internalization is a technology that allows light-induced delivery of DNA, drugs or other biological factors directly inside cells. Usually it requires that a photosensitizer be added to the drug-delivery system to photochemically destabilize the endosomal membrane. Here we present a system for *in vivo* DNA delivery in which these two components are assembled into one structure. This is a ternary complex composed of a core containing DNA packaged with cationic peptides and enveloped in the anionic dendrimer phthalocyanine, which provides the photosensitizing action. The ternary complex showed more than 100-fold photochemical enhancement of transgene expression *in vitro* with reduced photocytotoxicity. In an animal experiment, subconjuctival injection of the ternary complex followed by laser irradiation resulted in transgene expression only in the laser-irradiated site. This work demonstrates a new biomedical application for dendrimers, and the first success in the photochemical-internalization-mediated gene delivery *in vivo*.

There has been a strong incentive for the development of safe and effective gene vectors to achieve successful *in vivo* gene therapy[1–4]. Compared with viral vectors with an inherent risk for clinical use, non-viral synthetic vectors have received much attention owing to the advantages of safety, simplicity of use and ease of mass production[1–4]. A promising approach to the design of synthetic vectors is the use of cationic polymers and peptides. In general, the plasmid DNA (pDNA)/polycation complexes (polyplexes) are internalized by the cell through the endocytic pathway and need to be released from the endosome to deliver the genes to the nucleus. It is well known that this endosomal escape of the polyplexes is the main obstacle to obtaining efficient transfection[5]. Polycations possessing a buffering capacity, such as polyethylenimine (PEI), show a high *in vitro* transfection activity owing to the so-called proton sponge effect[5]; however, it is probable that the inherent cytotoxicity will impair their clinical utility as gene carriers. Hence, further efforts need to be devoted to the development of synthetic vectors especially for *in vivo* use.

In contrast, site-specific gene transfer to somatic cells is strongly desired; however, the existing vectors, including the viral and non-viral vectors, might have great difficulty in achieving *in vivo* transfection in a site-specific manner. In this regard, a different concept has been proposed[6–10], photochemical internalization (PCI): the cytoplasmic delivery of macromolecular compounds is enhanced by the photochemical disruption of the endosomal membrane using light and a hydrophilic photosensitizer. This smart concept is, in principle, applicable to the *in vivo* gene delivery in a light-sensitive manner[10]. However, the cytotoxicity is accompanied by photochemical reactions in the cell, and this might need to be reduced before considering further applications of this technology. Moreover, there is still room for optimization and modification

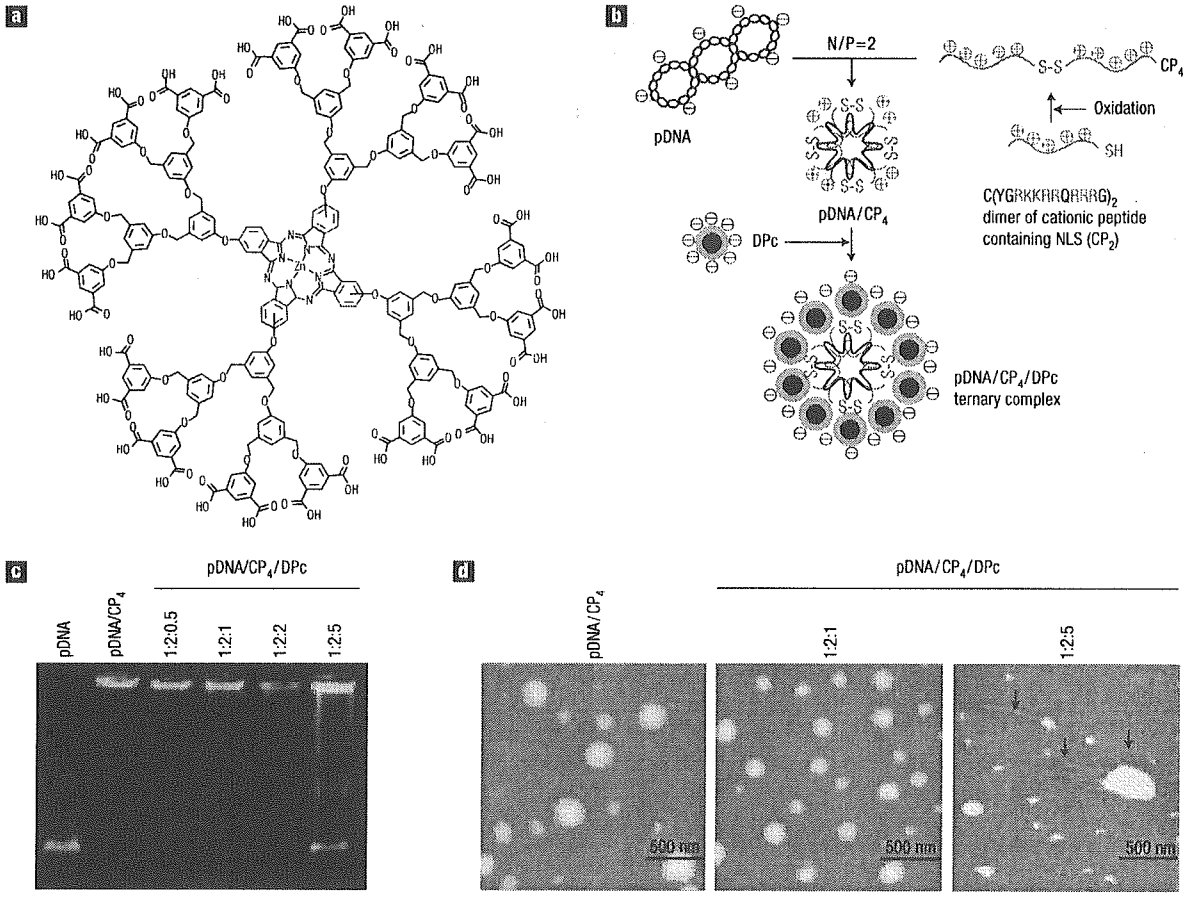

Figure 1 Preparation and characterization of the ternary complex. a, The chemical structure of ionic DPc. **b**, A scheme for preparation of the pDNA/CP_4/DPc ternary complex. **c**, Gel retardation assay of the pDNA/CP_4 polyplex prepared at an N/P ratio of 2, and the ternary complexes with varying charge molar ratios of pDNA/CP_4/DPc. **d**, AFM images of the pDNA/CP_4 and pDNA/CP_4/DPc complexes. Arrow heads indicate plasmid DNA released from the ternary complexes.

for *in vivo* applications. From the viewpoint of materials science, this concept can be integrated into nanodevices for drug and gene delivery.

In the present paper, we assume that the control of subcellular localization of photosensitizers may be a key to the PCI-mediated gene delivery with reduced cytotoxicity, because the photodamage to sensitive organelles other than the endosomal membrane, for example the plasma and mitochondrial membranes, might be responsible for the photocytotoxicity[11]. In addition, gene carriers should be equipped with a photosensitizing unit as one component for *in vivo* applications. These assumptions motivated us to develop a light-responsive gene carrier based on a ternary complex of pDNA, cationic peptides and anionic dendrimer-based photosensitizers (dendrimer phthalocyanine: DPc; Fig. 1a). Dendrimers, the three-dimensional tree-like branched macromolecules, have attracted growing interest as materials for drug and gene delivery[12–16], and the ternary complex is a different biomedical application of dendrimers. The ternary complex has shown significant photochemical enhancement of the transgene expression *in vitro* with reduced photocytotoxicity and *in vivo* gene transfer to the conjunctival tissue in the rat eye in a light-selective manner.

The ternary complex is composed of a core of a pDNA/cationic polymer polyplex enveloped with anionic DPc (Fig. 1a) as illustrated in Fig. 1b. DPc possesses a centre phthalocyanine molecule surrounded by a second generation of aryl ether dendrons, and 32 carboxyl groups on the periphery of DPc allow polyion complex formation with cationic polyplexes. In the present study, the core polyplex was formed from a quadruplicated cationic peptide (CP_4), where a peptide (CP_2: C(YGRKKRRQRRRG)$_2$)) was dimerized through a disulphide linkage, and pDNA was mixed with the CP_4 peptide at a molar ratio of cationic amino acids to a phosphate anion in DNA (N/P ratio) of 2. It has been demonstrated[17] that CP_2 and CP_4 contain a nuclear localization sequence (NLS) and thereby effectively mediate the gene transfection to the cell with the aid of conventional transfection reagents such as PEI and LipofectAMINE to promote the endosomal escape of the polyplex. Thus, these potent cationic peptides were used for the formation of the ternary complex to ensure the efficient gene transfection following the endosomal escape of the polyplex.

In this study, the ternary complexes were prepared by varying the charge molar ratios of pDNA/CP_4/DPc, and the complex formation was confirmed by a gel retardation assay (Fig. 1c). As a result, pDNA was incorporated into the complexes with charge ratios up to 1:2:2, but was excluded from the complex with a charge ratio of 1:2:5. The release of pDNA from the 1:2:5 complex was also observed by atomic force microscopy (AFM) as shown in Fig. 1d.

Table 1 Size, size distribution and ζ-potential of the electrostatic assemblies containing plasmid DNA.

	Cumulant diameter (nm)	Polydispersity index	ζ-potential (mV)
pDNA/PEI (1:10)	127.8	0.211	23.8±0.1
pDNA/CP_4 (1:2)	100.8	0.185	21.3±2.3
pDNA/CP_4/DPc (1:2:0.5)	149.7	0.115	−8.5±3.6
pDNA/CP_4/DPc (1:2:1)	130.8	0.108	−29.2±2.6
pDNA/CP_4/DPc (1:2:2)	107.7	0.143	−23.2±0.9
pDNA/CP_4/DPc (1:2:5)	267.1	0.180	−49.6±0.7
pDNA/CP_4/PAA* (1:2:0.5)	621.2	0.444	−27.1±0.8
pDNA/CP_4/PAA (1:2:1)	672.0	0.477	−25.8±0.4
pDNA/CP_4/PAA (1:2:2)	912.3	0.361	−24.3±0.8
pDNA/CP_4/PAA (1:2:5)	1426	0.278	−25.3±2.3

* PAA: Poly(aspartic acid) homopolymer with a polymerization degree of 26

Thus, addition of excess DPc might disintegrate the pDNA/CP_4 polyplex. The size, polydispersity index and ζ-potential of the pDNA/CP_4/DPc ternary complexes are summarized in Table 1. The addition of DPc to the positively charged pDNA/CP_4 polyplex gave negative ζ-potential values, suggesting the formation of ternary complexes covered with anionic DPc. A decrease in the size of the ternary complexes with increasing DPc ratios may be attributed to shrinkage of the cationic peptide corona on the polyplex surface through electrostatic interaction with DPc. Surface modification with anionic DPc provided the 1:2:1 and 1:2:2 complexes with excellent colloidal stability, whereas the 1:2:0.5 complex possessing an almost neutral ζ-potential value tended to precipitate in several hours. Significantly, the ternary complexes showed much lower polydispersity indices compared with the pDNA/CP_4 or PEI polyplexes (Table 1). The AFM observation has revealed consistently that the 1:2:1 complex consists of spherical particles with a narrow size distribution, which is in marked contrast to the pDNA/CP_4 polyplex containing large aggregates (Fig. 1d). Note that the addition of poly(aspartic acid) (PAA) homopolymer with a polymerization degree of 26 to the pDNA/CP_4 polyplex resulted in a large aggregate formation (Table 1). Hence, the three-dimensional structure of DPc is assumed to play an essential role in the formation of a ternary complex with a narrow size distribution and excellent colloidal stability. The layer-by-layer assemblies of oppositely charged polyelectrolytes onto colloidal particles have attracted considerable attention[18,19]; however, the pDNA/CP_4/DPc ternary complex is definitely discriminated from the layer-by-layer assemblies, because a core composed of hard materials is not required for the formation of the ternary complex. Thus, the ternary complex presented here is a supramolecular assembly consisting of a pDNA/CP_4 polyplex core and a DPc envelope.

The properties of DPc and the ternary complex related to the initial steps in the gene transfection to the cell (that is, processes from the cellular uptake to when photodamage to the endosomal membrane occurred) were evaluated, because the ternary complex was designed to control these processes. First, the cellular uptake of the ternary complex was evaluated by flow cytometry using a fluorescein-labelled pDNA, as shown in Fig. 2a. The amount of cellular uptake of the ternary complexes was less than that of cationic polyplexes such as pDNA/CP_4 and pDNA/PEI, and decreased as the DPc ratio increased. The ternary complex covered with anionic DPc should have a lower affinity for the negatively charged plasma membrane of cells, accounting for the results in Fig. 2a.

The pH-dependent hydrophilic/hydrophobic behaviour of DPc and its possible interaction with cell membranes was estimated by octanol/water partitioning, which is a common method for evaluation of drug–membrane interactions[20]. The partitioning (%) of DPc to the octanol phase increased as the pH decreased to 5.0–5.5 (Fig. 2b), suggesting the increased hydrophobicity of DPc and possible interactions with cell membranes under low-pH conditions. Because the DPc consists of a hydrophobic dendritic framework, the protonation of the peripheral carboxyl group under acidic conditions might increase its hydrophobicity. This result suggests that DPc may be released from the ternary complex under endosomal pH conditions to interact with the endosomal membrane, while electrostatically interacting with the positively charged surface of the polyplex at physiological pH. This assumption offers an interesting opportunity to selectively photodamage the endosomal membrane for effective PCI.

Figure 2c shows the subcellular distribution of FITC-labelled dextran co-incubated with the 1:2:1 ternary complex. It was demonstrated that FITC-dextran showed diffused fluorescence throughout the cytoplasm after photoirradiation, whereas it showed punctuated fluorescence corresponding to localization in the endosome and/or lysosome before photoirradiation. This result suggests the capability of the ternary complex of releasing the contents in the vesicular organelles to the cytoplasm on photoirradiation.

To evaluate the potential of the ternary complex for PCI-mediated gene delivery, *in vitro* transfection experiments were performed on HeLa cells with a luciferase (Luc) reporter gene in the presence or absence of photoirradiation. Simultaneously, the cell viability was assessed by MTT assay (see Methods). Figure 3a shows the transfection efficiency and cytotoxicity of the pDNA/CP_4 polyplex and pDNA/CP_4/DPc ternary complexes with varying charge ratios of DPc after irradiation of the light with increasing fluence. In this experiment, the cells were photoirradiated after 6-h incubation with each complex and fresh medium replacement, followed by 48-h post-incubation. The 1:2:1 and 1:2:2 ternary complexes achieved more than 100-fold photochemical enhancement of the transgene expression with minimal photocytotoxicity over a wide range of fluence (−3.6 J cm^{-2}), whereas the 1:2:5 ternary complex, having a disordered structure, showed the lowest transfection activity (Fig. 3a). Note that a further increase in fluence resulted in a significant increase in the photocytotoxicity of the ternary complexes (a 50–70% decrease in the viability at 5.4 J cm^{-2}; see Supplementary Information, Fig. S1). The transfection to a different cell line (that is, 293T cells) revealed similar photochemical enhancement of transgene expression by the ternary complexes, although the 1:2:1 and 1:2:2 ternary complexes showed appreciable photocytotoxicity at a fluence higher than 2.7 J cm^{-2} (see Supplementary Information, Fig. S2A). Furthermore, when HeLa cells were incubated with the ternary complexes for a prolonged period (that is, 24 h) before photoirradiation, the results were similar to those in Fig. 3a (see Supplementary Information, Fig. S2B). The effect of PCI-mediated transfection was comparable to or more effective than that of hydroxychloroquine, a potent endosomotropic agent[21], depending on the cell lines (see Fig. 3a and Supplementary Information, Fig. S2A).

The effect of the ternary complex on the PCI-mediated transfection was further compared with that of $AlPcS_{2a}$ (aluminium phthalocyanine with two sulphonate groups on adjacent phthalate rings), which was demonstrated to be an effective photosensitizer in PCI[8–10]. Figure 3b shows the effect of $AlPcS_{2a}$ on the transfection efficiency of the pDNA/CP_4 polyplex (N/P ratio = 2) and cytotoxicity to HeLa cells with varying concentrations of $AlPcS_{2a}$ and fluence. In the system using $AlPcS_{2a}$, the photochemical enhancement of the transfection was accompanied by a significant increase in the photocytotoxicity, regardless of the concentrations of $AlPcS_{2a}$. Comparison between Fig. 3a and b reveals that the ternary complex achieved an expanded range of safe light doses,